Electronically Reconfigurable and Tunable Fractional-Order Filter Using Resonator Concept and Feedforward Path for Low-Frequency Tone Signalization

ONDREJ DOMANSKY, ROMAN SOTNER[ID], **(Member, IEEE), LUKAS LANGHAMMER**[ID],
AND LADISLAV POLAK[ID], **(Member, IEEE)**
Department of Radio Electronics, Faculty of Electrical Engineering and Communication (FEEC), Brno University of Technology, 616 00 Brno, Czech Republic

Corresponding author: Ondrej Domansky (domansky@phd.feec.vutbr.cz)

ABSTRACT A novel electronically reconfigurable fractional-order filter allowing independent electronic frequency tuning and switchless change of the transfer response by a single parameter between standard band-pass, inverting all-pass response and special type band-reject response is presented in this work. The differences between these special transfer characteristics and standard features consist in magnitude and phase response behavior. Inverting amplification or attenuation is also available. The filter has tested frequency range between 1 Hz and 100 kHz. The proposed fractional-order filter (using two fractional-order element having equivalent capacity 8.7 uF/sec^1/4, $\alpha = 3/4$) tunability yields one-decade range approximately between 10 Hz and 100 Hz by transconductance between 0.19 and 1.1 mS (fractional-order design helps with reduction of driving force less than one decade). The application example in frequency/phase detector (operationability around center frequency 100 Hz - between 50 and 180 Hz) and further signaling frequency detecting system for frequency shift keying demodulator offers maximal detectable voltage (about 300 mV) for alignment (zero phase shift) of the signals of the same frequency (center frequency of the proposed filter in inverting all-pass mode). It also offers an interesting application in frequency shift keying demodulation process (or for identification/signalization purposes of certain frequencies) by usage of a simple additional comparator generating clear output state. Cadence simulations as well as experimental tests using integrated cells of special multipliers fabricated in ON Semiconductor 0.35 μm I3T25 CMOS process confirm operationability of the proposed concept as well as simple application of special response of the filter for phase/frequency detection and demodulation purposes.

INDEX TERMS Active filter, electronic adjustment, fractional order, operational transconductance amplifier, resonator, switchless adjustment, transfer response reconfiguration.

I. INTRODUCTION

In many cases, signal processing and readout systems require modification of transfer response (the type of transfer response, bandwidth limit, etc.). In such cases, only tunability or multifunctionality (manual selection of the output type of response by switches) is insufficient [1], [2]. Reconfiguration of the transfer response of a filter cannot be solved by standard active devices (operational amplifiers) because many degrees of freedom are expected (pass-band gain, pole frequency, etc.) [3].

Fractional-order (FO) circuits [4] bring new features to this field because areas between stop-bands and pass-bands can be set with less steepness than in integer-order cases. It is consequence of the magnitude slope dependence on frequency and its direct relation with the order of the FO devices used in the design [5]. Complex structures of many integrators in feedback loops [1], [2] offer reconfiguration of the slope of response by selection of an appropriate output of the integrator [5]. The full reconfiguration of transfer response (switchless change of transfer response) requires

---

more extensive modifications, degrees of freedom and coordination (suitable setting and simultaneous adjustment) of driving forces – DC voltages [6]. Specific requirements on the slope of response can be fulfilled by FO approaches [4]. These requirements depend on specific applications.

The following part of the work introduces corresponding topics and highlights advantages of the presented solution among already studied and analyzed concepts in the field of reconfigurable filters. Specific setting of the filter has an interesting and unusual application for frequency/phase detection. It is important to note that presented combinations of magnitude and phase responses are also unavailable in standard integer-order concepts (without reconfigurable features).

A. RECONFIGURABLE FILTERS

Reconfigurable filters [3] can be used with high benefits for equalization (modification and optimization of gains in various frequency bands based on current conditions of transmission environment or requirements of a system) of a communication channel. The most important feature of these types of filters consists in a single-input single-output topology.

The transfer response is not selected at several input or output terminals but established by appropriate setting of the parameters of topology (in many cases continuously). Several topologies in standard circuit theory (lumped elements) have been reported in [3] but significant attention is especially devoted to higher radiofrequency (RF) bands (GHz) due to the easiest construction of these devices (electromagnetically coupled elements). In these RF bands, the switchless change of transfer response can be easily solved even in passive solutions [7]–[11]. Research in this field especially targets on microwave systems. However, in the field of low-frequency applications, it is not an easy task. Special active elements having various degree of freedom (multi-parameter adjustability) and extensive complexity of active circuitry are required [5]. Microwave-based concepts use electromagnetic couplings existing in RF bands (higher than MHz), which is not easily available for low-frequency signals. These concepts have certain advantages of power consumption because majority of these circuits, except biasing of diodes for tuning [10], [11], does not require power supply [7]–[9]. However, very high geometrical accuracy of the designs must be ensured. In some cases, reconfiguration is given by micro-electro-mechanical systems (MEMS) based switches [9]. If there are electronic adjustable features (i.e. center frequency or bandwidth adjustment), they are concentrated to PIN diodes, varactors [10], [11] or even mechanical switches [9] that are not allowing continuous adjustment. In order to see conceptual differences, typical solutions using lumped elements as well as microwave approaches are compared in Table 1. The analysis of solutions, presented in Table 1, leads to the following conclusions:

a) resonators are not frequently used for design of reconfigurable filters in standard lumped elements-based

approaches (it is a significant domain of microwave circuits) [3]–[6];

b) the highest degree of reconfigurability of the filter requires a complex circuitry and multiparameter adjustable active elements [5], [6];

c) the adjustment of the order reconfiguration influences the slope between pass and stop band, without change of the transfer type [5];

d) the number of available transfer responses in microwave resonator based approaches is either quite low [7], [8], 10] or does not include band-pass (BP) response (it is the most frequently used response in many applications) [7], [8];

e) the adjustment of microwave filters has not electronic character [7]–[9], only several cases include some electronic adjustment employing variable capacity of diode (varicap) by bias voltage [10], [11];

f) transfer responses of special character (untypical behavior of magnitude and phase responses) together with simple amplification simultaneously) are not available and studied.

Important advantage of our concept consists in utilization of basic active devices without mutliparameter feature (allowing extended degree of freedom) but sufficient for expected purpose of electronic tunability and transfer reconfiguration. Based on Table 1, no design was target to low-frequency domain. Standard ideal integer-order LC resonator cannot be used in the presented solution because of instability when certain conditions are fulfilled. Therefore, some settings of the presented circuit, using integer-order elements, will cause instable operation (BP response especially). On the other hand, the utilization of FO elements makes the solution stable. The main results of the analysis of solutions indicated by Table 2 show the following:

a) there is no relation between reconfiguration of transfer responses and variation of parameters of FO device when a passive FO device is used [6], [15], [16];

b) electronic tuning (center, pole frequency) does not require modification of the set of parameters when a passive FO device is used [6], [15];

c) the passive FO device must be completely replaced when the change of order is required [6], [15], [16];

d) electronic tuning requires modification of the set of parameters when active solution of FO filter (the FO character is approximated by higher-order filter response [13]) is used [13], [14];

e) active solution of FO character offers electronic setting of the order [12]–[14], [17] but topology is very complex (many active elements [13], [14]) requiring many degrees of freedom of many parameters [13], [14];

f) electronic adjustment of stop-band attenuation (in order to set useful as well as undesirable spectral components properly) of the BP response is not solved in the reported cases;

g) previous solutions do not use resonator concept;

h) in some works [12], [14], [17], the number of transfer responses is quite low;

i) the input impedances are not high and output impedances are not low simultaneously in several promising structures (for immediate application in voltage mode) [6], [13]–[15]. However, it cannot be considered as a direct disadvantage in current-mode solutions [5].

Very often, solutions approximating FO Laplace operator have a complex topology [13], [14], [18], [19]. However, it is a cost for beneficial reconfigurable features (tuning and transfer response reconfiguration) of the filter (electronically). Reconfiguration of the order and transfer function is also available in works [18], [19] but solved by switches and decoders discontinuously. Therefore, these solutions are excluded from Table 2 where continuously electronically adjustable solutions are compared.

The most important drawback of recently reported multifunction solutions consists in necessity of new set of values of parameters (matching for simultaneous change) for each change (readjustment) of the order. Therefore, utilization of the resonator concept in FO designs brings significant advantage. The FO device has fixed features – passive RC approximation) and responsibility for tuning concentrates to active elements except operational amplifiers (they offer complex and non-tunable solution of resonator [20]). The operational transconductance amplifiers (OTAs) [21] are used in our case. Moreover, the adjustment of the order can be separated from tuning when the FO device is replaced by active solution [13]. A simple core of the useful reconfigurable filtering topology, allowing special transfer functions, can be created by a simple resonator structure. There were reported several examples of fractional-order LC resonators (see Table 3) but they have some disadvantages (e.g. linear electronic tuning is not allowed [22]–[25] and high complexity [26], [27]) reported in detailed comparison in [22]–[27]. Their basic principle utilizes standard Antoniou gyrators [20] with operational amplifiers for not easily tunable passive solutions and electronically adjustable OTA-based gyrator [21]. Different circuit solutions of the gyrator were obtained by current conveyors and optocouplers for electronic adjustment [27]. Our modification in the topology of [21], used in this work, brings new linear voltage control of transconductance (OTAs are created by linear multipliers) where the value of transconductance has no lower limit (can be even zero). Topology in [26] offers electronically readjustable order of the FO resonator (equivalent inductance, capacity or both). However, this useful feature results in complexity of the concept.

B. PHASE DETECTOR
Standard concepts of phase detector in frequency demodulators employ integer-order band-pass filters using basic passive elements (LC) having non-tunable properties. The phase detector solves especially phase relation between the input and reference waveforms. On the other hand, the values of amplitude have also significant influence because they determine the value of DC (or low-frequency) voltage given by the value of phase shift. In the case of standard integer-order RC and LC filters in the phase shifting path, the magnitude changes with ±20 dB/dec around the center frequency of the filter. It may have significant impact on the DC output level and accuracy of phase shift evaluation, especially for large values of phase shift changes where magnitude response varies significantly. The presented technique offers a simple solution for the issue with magnitude increase/decrease in the input path of frequency demodulator providing phase shift for input waveform with varying frequency. Our application example shows utilization of one selected and set transfer response (inverting AP response) in phase/frequency detecting circuit. Phase and frequency detectors may find applications in many areas including communication systems [28]–[32] and low-frequency biomedical technologies [33]. Electroencephalogram (EEG) and electrocardiogram (ECG) signal readouts appreciate operation of these applications in units-hundreds of Hz [33]. Comparison of typical concepts in Table 4 shows usefulness of solutions from both topological (complexity) and performance aspects. The filters used in works [28]–[32] do not have flat magnitude responses ensuring constant amplitude for both incoming signals for multiplication. In addition, also overall complexity of detectors is larger in many works [29]–[32] than in our case. Electronic tuning of the filter brings useful feature because the operation (carrier) frequency can be easily changed (impossible in [29]) and not documented in the rest of works [28], [30]–[32]). The last work [34], regarding to this topic, has very similar features. However, there are significant differences. In this paper, the multiplier has a single output (the type of multiplier in this work and in [34] is different and has different internal CMOS topology, i.e. the doubled output voltage is not available here (not necessary here – sufficient dynamical ranges of active devices) but the topology is simpler than in [34]). Next, there is difference in the phase response of the ''filtering'' block in the frequency/phase detector. Work [34] uses a standard first-order all-pass response ($0° \rightarrow 180°$) whereas solution in our actual work employs a special response of fractional-order reconfigurable filter generating inverting all-pass response having phase limits in $\pm180°$ ($+180° \rightarrow -180°$) with $0°$ at the target value of the detected frequency (the same as compared). It results in the maximal detected output voltage of the multiplier when the phase difference of signals of the same frequency is zero (or the input frequency of complete phase detector is identical with the setting of the filter). On the other hand, the behavior of phase detector in [34] is different. The maximal output DC voltage is available for the largest phase/frequency difference, zero voltage for alignment of the input and reference waves. The overall complexity of both circuits is similar and in [34] the power consumption is lower than in our presented solution (given by the used technology and supply voltage).

TABLE 1. General comparison of principles of filters having a feature of transfer response reconfiguration.

Reference	Solution of the filter based on resonator	Purpose	Principle	Transfer response switchless reconfiguration in the same topology without change of the FO device character	Integer order of the filter (when applicable)	Fractional-order tested (value of the order of used FO device)	Electronic adjustment (driving force)	Number of transfer response available	Type of transfers	Symmetrical magnitude slope of band pass response	Special phase responses available	Complexity (number of active / passive devices)	Complex active device (multiparameter adjustability) not required	Only grounded capacitors (or FO elements) required	Useful feature among standard tuning	Supply and power consumption	Experimentally tested (with fabricated IC)
[3]	No	Middle frequency	Multi-feedback loops	Yes	2	No	Yes	6	AP, BR, HP, iBP, HPZ, LPZ	Yes	No	4 / 2	Yes	Yes	Transfer reconfiguration	±5 V, (N/A)	Yes (No)
[5]	No	Middle frequency	Multiple leap-frog feedback	Yes	4	Yes (0.3→0.7)	Yes	1	LP of 1.-4. order	-	No	> 5 / 4	Yes	Yes	Order reconfiguration	±1,65 V, (N/A)	Yes (Yes)
[6]	No	Middle frequency	Multi-feedback loops	Yes	2	Yes (0.3→0.7)	Yes (current)	4	LP, HP, BP, BR	No	N/A	5 / 4	No	No	Transfer reconfiguration	±1,65 V, (N/A)	No (No)
[7]	Yes	High frequency	RF coupled resonators	N/A	2	N/A	No (resonator geometry-mechanical)	2	AP, BR	-	N/A	*	**	N/A	Transfer reconfiguration	**	Yes (N/A)
[8]	Yes	High frequency	RF coupled resonators	N/A	N/A	N/A	No (resonator geometry-mechanical)	2	AP, BR	-	N/A	N/A	**	N/A	Transfer reconfiguration	**	No (N/A)
[9]	Yes	High frequency	RF coupled resonators	N/A	3	N/A	***	3	BP, AP, BR	Yes	N/A	N/A	**	N/A	Transfer reconfiguration	**	Yes (N/A)
[10]	Yes	High frequency	RF coupled resonators	N/A	N/A	N/A	Yes (voltage)	2	BP, BR	Yes	N/A	- / >10	**	N/A	Transfer reconfiguration	**	Yes (N/A)
[11]	Yes	High frequency	Phase shifter + band-pass filter	Yes	1	N/A	Yes (coupled transmission lines)	3	BP, BR, DT	Yes	N/A	N/A	**	N/A	Transfer reconfiguration	**	Yes (N/A)
									Proposed								
Fig. 1	Yes	Low frequency	LC resonator + summation with adjusted input signal	Yes	2	Yes (0.75)	Yes (voltage)	4	BP, iAP, sBR, iDT	Yes	Yes	5 / 3	Yes	Yes	Transfer reconfiguration	±1,65 V, (40 mW)	Yes (Yes)

N/A – not available; s – special (nonstandard); middle frequencies: kHz – MHz; low-frequencies: Hz – kHz; high-frequency: MHz – GHz;
*planar substrate layers; ** passive; *** resonator geometry – mechanical + micro-electro-mechanical-system (MEMS);
AP – all-pass, BR – band reject, BP – band-pass, HP – high-pass, LP – low-pass, DT – direct transfer response (i – inverting, Z – with transfer zero)

C. CONTRIBUTION OF THIS WORK

Based on the above discussions, the main contribution of this work is in the design of a novel type of reconfigurable filter using specific electronically adjustable feedforward path and electronically adjustable resonator. Among others, the new feature of the filter consists in simultaneous availability of BP (order of passive FO elements allowing the set of magnitude slope of attenuation), inverting all-pass (iAP), and special band-reject (sBR) response having a common magnitude response and special phase response not available in standard range between $0 \rightarrow \pm 90°$ (integer order case – 2nd order circuit) but in range of $+180° \rightarrow -180°$. The proposed filter offers features (available simultaneously) which are not standardly available and discussed in similar solutions:

a) several types of magnitude and phase responses available by electronic reconfiguration (single parameter);
b) stable operation of LC resonator without dumping (impossible in ideal integer-order systems – issues with stability);
c) a resonator-based concept excluding utilization of floating passive elements;
d) a concept useful for specific demand on the slope of attenuation (fitting for FO circuit applications – cannot be solved by integer-order circuits);
e) high input and low output impedances and
f) electronically adjustable active devices (OTAs) that allows to set both polarities of transconductance (useful in reconfigurable systems) for complete electronic control (tuning, switchless transfer response configuration) of the proposed filter. Note that the presented method of transfer response reconfiguration does not suppose any change (modification) of the FO device (independent on the order and inductive or capacitive character).

The application example in phase/frequency detection (for demodulation or synchronization purposes) indicates a simple circuitry and easily electronically tunable input/carrier frequency. Therefore, features of the system can be easily modified.

D. ORGANIZATION

This paper is organized as follows. Introductory section shows comparison of the proposed solution and its application with hitherto published works and explains motivation and contribution of this work. Section II introduces the proposed concept and its principle. Section III describes the used active elements. Experimental verification of the proposed filter and its application is presented in Section IV. Section V concludes this work.

II. PROPOSED SOLUTION OF SPECIAL FRACTIONAL-ORDER FILTER

The FO filter, shown in Fig. 1, offers reconfigurable features that are useful for further applications. The proposed topology includes two feed-forward branches performing adjustable inverting amplification and tunable FO band-pass filter based on an LC resonator. The sum of both branches creates the target reconfiguration. This technique is similar to the so-called Shadow filter operation [35] (difference is in the orientation of loop transfer) and it represents certain alternative targeting on the reconfiguration of transfer

TABLE 2. Specified comparison of lumped elements based recent switchless transfer response electronically reconfigurable (continuously) fractional-order active filters.

Reference	Year of publication	Continuous electronic tuning of filter (center frequency) documented	Matching of set of parameters not required for frequency tuning	Electronic continuous switchless reconfiguration of response (driving force) in the identical topology	Number of available transfer responses	Type of transfers	Symmetrical (magnitude slope) BP presented	Topology based on resonator	Special magnitude and phase responses available	Single parameter continuous electronic adjustment of stop-band attenuation of BP response possible	Solution of FO device (or approximant of Laplacian operator)	Transfer response reconfiguration without change of the FO device properties	New set of parameters not required for order change	Electronic setting (continuous) of the order	Number of active / passive devices	Grounded capacitors (or FO elements) required	High input impedance, low output impedance	Supply and power consumption	Experimentally tested (with fabricated IC devices)
[6]	2019	Yes	Yes	Yes	4	LP, HP, BP, BR	No	No	No	N/A	Passive (RC approximant)	Yes	Yes	No	5 / 4	Yes	No, No	±1.65 V, (N/A)	No (No)
[12]	2010	Yes	N/A	N/A	2	LP, HP	N/A	No	No	N/A	Active	N/A	No	Yes	*	-	Yes, Yes	N/A, (N/A)	Yes (No)
[13]	2017	Yes	No	Yes	4	LP, HP, BP, BR	Yes	No	No	No	Active	N/A	No	Yes	7/11 / 2/4	Yes	Yes, No	1.5 V, (N/A)	No (No)
[14]	2017	Yes	No	Yes	2	HP, LP	N/A	No	No	N/A	Active	N/A	No	Yes	7 / 3	Yes	No, No	N/A, (N/A)	Yes (No)
[15]	2019	Yes	Yes	Yes	4	LP, HP, BP, BR	No	No	No	Yes	Passive (RC approximant)	Yes	Yes	No	6 / 2	No	No, No	N/A, (N/A)	Yes (Yes)
[16]	2017	No	-	Yes	3	iDT, iHP, AP	N/A	No	No	N/A	Passive (RC approximant)	Yes	Yes	No	2 / 2	Yes	Yes, Yes	±5 V, (N/A)	No (No)
[17]	2020	No	N/A	Yes	2	LP, HP	No	No	No	N/A	Active	N/A	No	Yes	*	-	Yes, Yes	5 V, (1 W)	Yes (No)
Proposed																			
Fig. 1	2021	Yes	Yes	Yes	4	BP, iAP. sBR, iDT	Yes	Yes	Yes	Yes	Passive (RC approximant)	Yes	Yes	No	5 / 3	Yes	Yes, Yes	±1.65 V, (40 mW)	Yes (Yes)

Active solution of FO device = approximation by filter or bilinear segments; * solved as programmable analog array;
N/A – not available; s – special (nonstandard); AP – all-pass; BR – band reject; BP – band-pass; HP – high-pass; LP – low-pass; DT – direct transfer response (i – inverting, Z – with transfer zero)

responses more than on quality factor adjustment in Shadow filter design [35]. However, to the best of authors' knowledge, this approach was not presented with advantages that are discussed in this paper.

The circuit topology uses OTAs [21], [36], [37] and voltage differencing differential buffer (VDDB) [36], [37] for summing operation. The LC resonator employs an OTA-based gyrator (immittance converter and inverter [21]) where passive RC approximants of the FO passive device (constant phase element) [38]–[40] are employed (see Fig. 2). Such an implementation offers simple electronic tunability of the pole (center) frequency of the filter. Note that several attempts with sum of simple fractional and integer-order responses (integrators, differentiators) and resulting features were already studied [41], [42]. However, this work is different from previous studies due to the presence of full resonator allowing adjustable features in the topology together with adjustable feed-forward path. Considering the gain of the amplifier $A = g_{m4} \cdot R$ (and equal order α of both FO elements in topology), the complete circuitry of reconfigurable filter in Fig. 1 has the following transfer function:

$$K_f(s) = \frac{s^{2\alpha} L_\alpha C_\alpha A + s^\alpha L_\alpha \cdot g_{m1} + A}{s^{2\alpha} L_\alpha C_\alpha + 1}$$
$$= \frac{s^{2\alpha} L_\alpha C_\alpha g_{m4} R + s^\alpha L_\alpha \cdot g_{m1} + g_{m4} R}{s^{2\alpha} L_\alpha C_\alpha + 1}, \quad (1)$$

where simple electronic adjustability and tunability of resonant frequency can be obtained by replacement of L_α (see Fig. 2) by synthetic equivalent [21]:

$$Z_{L\alpha} = s^\alpha L_\alpha = s^\alpha C_\alpha \frac{1}{g_{m2} g_{m3}} \cong s^\alpha C_\alpha \frac{1}{\left(k \cdot V_{SET\_gm2,3}\right)^2}, \quad (2)$$

where parameter k represents transconductance constant of the used multiplier/OTA. Then, (1) can be modified to:

$$K_f(s) = \frac{s^{2\alpha} C_\alpha^2 g_{m4} R + s^\alpha C_\alpha g_{m1} + g_{m2} g_{m3} g_{m4} R}{s^{2\alpha} C_\alpha^2 + g_{m2} g_{m3}}. \quad (3)$$

The first available transfer – BP response is obtained for $A = g_{m4} \cdot R = 0$ (i.e. $g_{m4} = 0$):

$$K_{BP}(s) = \frac{s^\alpha L_\alpha \cdot g_{m1}}{s^{2\alpha} L_\alpha C_\alpha + 1} = \frac{s^\alpha C_\alpha g_{m1}}{s^{2\alpha} C_\alpha^2 + g_{m2} g_{m3}}. \quad (4)$$

The magnitude response has slopes defined by order of CPE ($\alpha \cdot 20$ dB/dec and phase response crosses 0 ° and reaches limits $\pm \alpha \cdot 90°$ as visible in Fig. 3 for $A = 0$).

Transfer response changes to sBR filter character when $A = -1$ ($g_{m4} = 1/R$) having standard BR magnitude response but phase response having different shape than expected for standard BR (see Fig. 3):

$$K_{sBR/iAP}(s) = -\left(\frac{s^{2\alpha} L_\alpha C_\alpha - s^\alpha L_\alpha \cdot g_{m1} + 1}{s^{2\alpha} L_\alpha C_\alpha + 1} \right)$$
$$= -\left(\frac{s^{2\alpha} C_\alpha^2 - s^\alpha C_\alpha g_{m1} + g_{m2} g_{m3}}{s^{2\alpha} C_\alpha^2 + g_{m2} g_{m3}} \right). \quad (5)$$

Symbolical representation (5) fits for iAP filter, but magnitude response has a character of BR filter. The phase responses of sBR has untypical behavior and phase range (see Fig. 3 and Section IV). The behavior for the value of A between 0 and -1 has very important consequences. The required value of A (negative) can be obtained by the multiplicative feature of the used specific OTA solutions or by proper polarity of transfer function (polarity of terminal selected for input of the OTA). The transfer response of inverting/noninverting follower or amplifier (abbreviated as inverting direct / direct transfers - iDT/DT) can be obtained for $A < 0$ ($A > 0$ respectively) and $g_{m1} = 0$ mS (available by multipliers).

Detailed study of (1) and variation of A between 0 and -1 by analytical form is not providing an easy survey. Therefore, a graphical solution of the ideal magnitude equation of (1) was prepared for specific condition of center frequency, which is derived below. This evaluation supposes the following definitions. The low-frequency and high-frequency band is determined by A when $s = j\omega \rightarrow 0$ or ∞, which is clearly

TABLE 3. Comparison of fractional-order resonators.

Reference	Electronic tuning	Linear dependence on driving force	Matching of parameters for electronic tuning not required	Voltage adjustment	Number of active / passive elements	Solution of FO elements	Electronic change of the order by set of parameters	Solved with fabricated IC devices
[22]	No	*	*	No	2 / 5	Passive	No	No
[23]	No	*	*	No	2 / 5	Passive	No	No
[24]	No	*	*	No	2 / 5	Passive	No	No
[25]	No	*	*	No	2 / 5	Passive	No	No
[26]	Yes	Yes	No	No	8 / 2	Active	Yes	Yes
[27]	Yes	Yes	Yes	Yes	4 / 5	Passive	No	No
Fig. 5	Yes	Yes	Yes	Yes	2 / 2	Passive	No	Yes

* standard Antoniou gyrator using operational amplifiers [20]

TABLE 4. Comparison of typical frequency/phase detectors.

Reference	Year of publication	CMOS process	Supply [V]	Power consumption [mW]	Purpose of concept	Oscillator not required in phase detection circuit	Type of used filter in structure	Ideal magnitude response of the filter is flat for all frequencies	Constant amplitude of both signals for multiplication	Detector tunable electronically for different operational (carrier) frequency	Overall complexity of phase detector (number of parts)	Overall complexity of detector (number of blocks)	Tested a processed signal levels in structures	Input dynamical range of used multipliers (OTAs) or any used element reported [mV]	Dependence of detected output voltage on phase difference shown	Maximum output voltage for zero phase difference	Experimental tests
[28]	2020	N/A	N/A	N/A	Radio-freq. systems (GHz)	No	low-pass	No	No	N/A	2	N/A	units of V	N/A	No	N/A	No
[29]	2014	0.13 µm	3.3	0.82	Middle frequency (tens of MHz)	No	RLC band-pass	No	No	No	2	3	units of V	N/A	No	No	No
[30]	2011	0.13 µm	1.2	0.26	Radio-freq. data reciever (GHz)	No	low-pass	No	N/A	N/A	2*	3	low hundreds of mV	N/A	No	N/A	Yes
[31]	2021	0.045 µm	2	485	Radio-freq. systems (GHz)	No	low-pass	No	N/A	N/A	2*	4	hundreds of mV	N/A	No	N/A	No
[32]	2017	0.13 µm TSMC	1.8	29	Radio-freq. systems (GHz)	N/A	low-pass	No	N/A	N/A	11	4	N/A	N/A	No	N/A	No
[34]	2021	0.18 µm TSMC	±0.9	5.7	Low-frequency (tens of kHz)	Yes	non-inverting all-pass	Yes	Yes	Yes	2	2	hundreds of mV	±200	Yes	No	Yes
Fig. 5	2021	0.35 µm ON	±1.65	47	Low-frequency (tens of kHz)	Yes	inverting all-pass	Yes	Yes	Yes	2	2	hundreds of mV	±500	Yes	Yes	Yes

* phase detector + LP (loop) filter for low frequency or DC output in case of phase locked loop application

visible from (1). The center frequency transfer is given as a modification of (1) where frequency dependent terms are substituted by center frequency:

$$\omega_p = \left(\frac{1}{C_\alpha L_\alpha}\right)^{\frac{1}{2\alpha}} = \left(\frac{g_{m2}g_{m3}}{C_\alpha^2}\right)^{\frac{1}{2\alpha}}\Bigg|_{g_{m2}=g_{m3}=g_{m23}}$$

$$= \left(\frac{g_{m23}}{C_\alpha}\right)^{\frac{1}{\alpha}}, \qquad (6)$$

to the form:

$$K_f(\omega = \omega_p) = \frac{j^{2\alpha}A + j^\alpha\sqrt{\frac{L_\alpha}{C_\alpha}}g_{m1} + A}{j^{2\alpha} + 1}$$

$$= \frac{j^{2\alpha}A + j^\alpha \frac{g_{m1}}{\sqrt{g_{m2}g_{m3}}} + A}{j^{2\alpha} + 1}. \qquad (7)$$

Graphical analysis is more effective and illustrative than complex and extensive formulas. We are searching for a point

where the magnitude of $|K_f|$ of the limits (for $\omega \to 0$ and ∞) equals to the gain of the BP filter at center (pole) frequency. Our theoretical discussion supposes two identical FO devices: $C_\alpha = 8.7~\mu\text{F/sec}^{1/4}$ ($\alpha = 3/4$) and center frequency 100 Hz ($\omega_p = 2\pi \cdot 100$, i.e. $g_{m2} = g_{m3} = g_{m23} = 1.1$ mS). Exemplary results and solution of this case are shown in Fig. 4. The point of intersection of lines of $|K_f~(\omega \to 0~(\infty))|$ and $|K_f~(\omega \to \omega_p)|$ yields $A = g_{m4} \cdot R = -0.6$. Then iAP response is obtained. Results in Fig. 4 indicate magnitude levels in low-frequency (0), high-frequency (∞) and center frequency (ω_p) positions for variation of A. The specific value of A, valid together for all three cases, yields almost constant (very small ripple) overall magnitude response of the filter (it is useful for further application). The specific configuration of the circuit allows for us to obtain a sBR filter response (phase response similar to standard iAP response in integer-order circuit) in the FO system, that cannot be commonly achieve by standard design approaches. The magnitude has
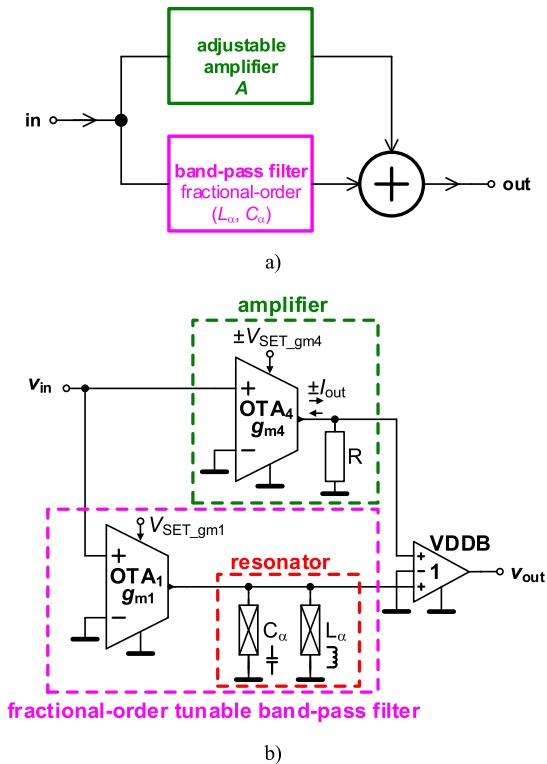
FIGURE 1. **Proposed approach of reconfigurable fractional-order filter: a) block principle, b) specific scheme available by standard circuit components.**

typical minimum (transfer zeros) but the phase response is not achieving the range of $0 \to \pm 90°$ but $+180° \to -180°$ (typical for iAP). From the results is clear that the center ("linear") member of numerator of (3) or (5) respectively is not disappearing from equation as in standard integer-order case for 2nd-order BR responses. Traces (linear in interesting range) and coordinates in Fig. 3 depend on the order α, next on the values of g_{m1} and g_{m23} (L_α value) but not on the value of C_α as visible in (7). An illustrative example of ideal transfer responses for stepped A in (1) is shown in Fig. 3 (including standard ideal BR response in order to see differences from sBR). Note that the following behavior will not be available in standard integer-order circuits because standard second-order circuits (LC resonator, etc.) have unstable operation (without dumping lossy resistor as a part of LC resonator) when the linear term of denominator is missing in transfer equations (see green and black traces in Fig. 3). Integer-order example (illustrative only) in Fig. 3 is obtained for $C = 8.7 \ \mu F$ and $g_{m23} = 5.47$ mS at center frequency of 100 Hz.

III. DESCRIPTION OF ACTIVE DEVICES
The presented concept employs two types of active elements fabricated in 0.35 μm I3T25 ON Semiconductor 3.3 V (± 1.65 V in our case) CMOS process. Principles of both devices with basic ideal definition of operation are shown Fig. 5. Figure 5 a) shows OTA formed by multiplier with two differential inputs and single current output. The transconductance constant has typical value $k = 1.8$ mA/V^2
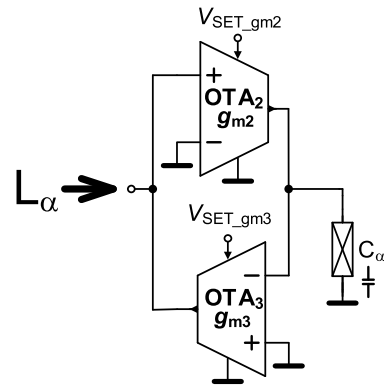
FIGURE 2. **Adjustable immittance inverter and converter based on OTAs.**

in Cadence Spectre simulations and 1.3 mA/V^2 in real experiments (expectable range of fabrication dispersion). The range of experimentally tested transconductance reaches $0 \to \pm 1.2$ mS (the multiplier-based concept allows to achieve a value of 0) for $V_{SET\_gm} = 0 \to \pm 0.7$ V. The bandwidth of g_m reaches more than 30 MHz for all conditions of tests [43], [44]. The dynamical range is supposed as linear for the input voltage higher than ± 0.5 V, where the total harmonic distortion (THD) falls between 0.1 and 1.5%. The terminal resistances of voltage inputs are higher than 100 MΩ and more than 100 kΩ for the current output. VDDB creates a simple sum and subtraction operation as it is captured in Fig. 5 b). The frequency response of unity-gain has a 3 dB drop at value higher than 45 MHz (all inputs). The input dynamical range reaches more than ± 0.7 V with THD below 1% (0.1% obtained for 500 mV$_{p-p}$). The voltage input resistances are higher than 100 MΩ and the voltage output resistance has a value lower than 0.4 Ω. More details can be found in [43] and [44]. The power consumption of the single multiplier and single VDDB reaches 7.8 mW and 9.1 mW respectively.

IV. EXPERIMENTAL VERIFICATION
The proposed filter was tested in simulations as well as in experiments by AC analysis. Furthermore, the filter has been utilized in a complex application example and tested in time domain. The application targets on simple frequency detection by a multiplier-based circuit. The RC approximant, so-called constant phase element (CPE) [38], [39], of the FO element ($C_\alpha = 8.7 \ \mu F/sec^{1/4}$, $\alpha = 3/4$) is plotted in Fig. 6. The bandwidth of constant phase range should reach at least 1 Hz – 100 kHz (tested experimentally) and the phase ripple in this band is maximally $\pm 2°$. The design of this device was performed by Valsa algorithm [38]–[40]. Note that traces (in figures) marked as "ideal" were gained from simulations with ideal active elements (modeled by controlled sources) and traces marked as "theory" are based on the discussed theoretical equations.

The values of parallel RC segments depend on the target value of equivalent capacity/inductance (pseudocapacity in our case) and on the order. The design has scalability of
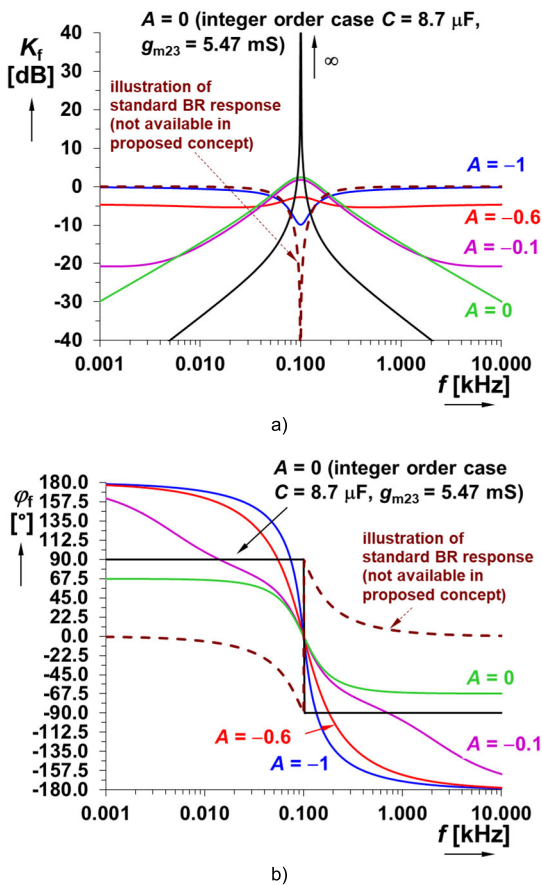
a)

b)

FIGURE 3. Illustration example of ideal behavior of the reconfigurable fractional-order filter: a) magnitude responses, b) phase responses.
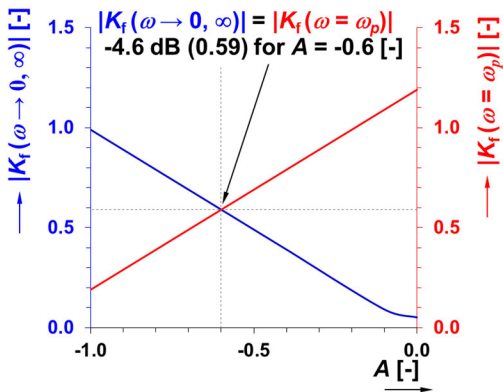

FIGURE 4. Searching for optimal value of gain A ($g_{m4} \cdot R$) giving almost flat magnitude response of the reconfigurable filter.

pseudocapacity (C_α) because not only the order but also the value of pseudocapacity is important for designers and final application. The values of the lowest "low-frequency RC segment" as well as the highest "high-frequency RC segment" have extreme values when extremely wideband (many decades, in our case theoretically from 1 Hz up to more than 5 MHz) operation and very low value of pseudocapacity (more than units of μF/sec$^{1-\alpha}$) of CPE solution are required. Our design presents a wideband CPE supposed

as universal for many tests and solutions (not optimized for specific application) having quite large value of pseudocapacity (i.e. low impedance levels at lowest frequencies). It also helps in the designs using active elements having low values of terminal impedances (real parts for example around 50-100 kΩ) in order to prevent real parasitic effects in the intended bandwidths. Different magnitude impedance plots are easily available but magnitudes higher than 100 kΩ are significantly influenced by real properties of active devices (many integrated as well as commercially available operational amplifiers have terminal impedances typically in hundreds and units of MΩ). However, many frequency-selective applications (e.g. filters and oscillators) have also similar selective requirements on the validity of CPE approximation (bandwidth of constant phase zone). In many cases, tunability of standard active filters is not significantly larger than one decade (based on available ranges of adjustable parameters of active elements). Therefore, also bandwidth limitation of CPE operation may be acceptable and significantly decreases complexity of the solution (number of RC segments). On the other hand, in our case, the low-frequency design still requires "borderline" values of RC segments (large R - MΩ, large C – μF), but the high-frequency segments can be removed. Experimental tests indicate that sufficient number of segments in our application and presented bandwidth can be reduced to half of original complexity (see Fig. 6). As it was explained, the complete circuit in Fig. 6 serves also for different purposes in different bandwidths. Therefore, its design respected universal application. The exact value of passive elements was obtained by serial/parallel combinations of partial elements (SMD elements can be placed and soldered in so called sandwich form). The electronic adjustment of the order and equivalent value of CPE is possible in active form by various methods [12]–[14], [17] (the chain of bilinear sections allowing the set of zero-pole adjustments was discussed for example in [41]) after simple modification – voltage to current converter and feedback modifying two-port/filter into impedance. However, it always results in significant increase of complexity and also unsynchronized readjustability of many active parameters.

A. TESTS OF THE FILTER
The parameters of the filter were set for pole-center frequency $f_p = 100$ Hz (gain $A = g_{m4} \cdot R$ varies for obtainment of iAP, BR, sBP and iDT responses). Ideal calculation of the features (for ideal results see Fig. 3) of the filter is given in Section II ($g_{m2} = g_{m3} = g_{m23} = 1.1$ mS, $g_{m1} = 1$ mS, $R = 1$ kΩ, $g_{m4} = -1.1, -0.6, -0.1$ and 0 mS). Note that there is no specific filter approximation selected.

The AC analysis was performed for all possible configurations of the filter. The results of analysis including all necessary parameters and driving voltages are shown in Fig. 7. The frequency responses show evident dependence of stop-band gain in low- and high-frequency corners. The inverting amplifier/follower (iDT only; DT has difference in phase response only) was verified for $A = -1.1$ ($g_{m4} = 1.1$ mS) and

$$i_o = (v_{X1} - v_{X2}) \cdot (v_{Y1} - v_{Y2}) \cdot k = (v_+ - v_-) \cdot g_m = (v_+ - v_-) \cdot V_{SET\_gm} \cdot k$$

a)

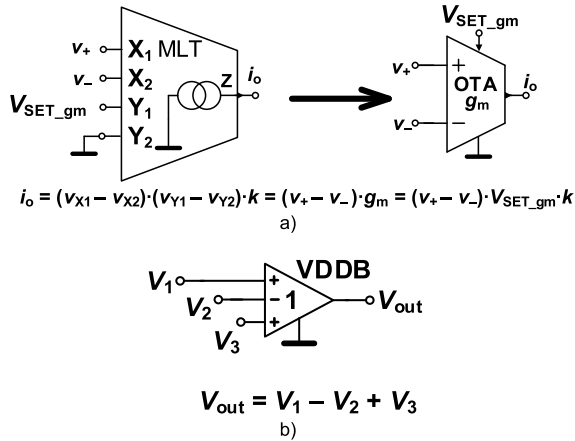$$V_{out} = V_1 - V_2 + V_3$$

b)

FIGURE 5. Principle of operation of active devices used for construction of the special fractional-order reconfigurable filter and its application: a) analog multiplier for application as OTA, b) voltage differencing differential buffer.
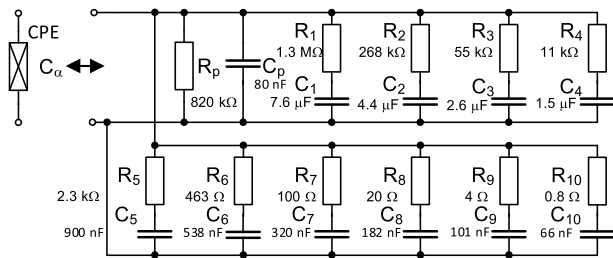

FIGURE 6. RC approximant of constant phase element used in experiments ($C_\alpha = 8.7 \ \mu F/sec^{1/4}$, $\alpha = 3/4$).

$g_{m1} = 0$ mS as visible in Fig. 8. The function of amplifier can be obtained for the same setting where A will be positive. The ideal traces in Fig. 8 a) and b) were obtained by simulations with ideal controlled sources representing active elements. The DSOX-3024T oscilloscope has been used (option of frequency response analysis) for all AC analyses below (the amplitude of the input signal is equal to 100 mV). The filter has center-frequency tunable properties covered by synthetic form of L_α ($g_{m2,3}$), see (6). However, this adjustment also varies with pass-band gain. Therefore, g_{m1} must be varied simultaneously too ($g_{m1} = g_{m2} = g_{m3} = g_{m123}$). The driving of g_m (allowed in specified range $0 \rightarrow \pm 1.2$ mS ensures at least one-decade tunability (required $g_m = 0.19 \rightarrow 1.1$ mS, i.e. $V_{set\_gm123} = 0.11 \rightarrow 0.61$ V) and adjustment of gain of the feedforward path of the filter at least $0 \rightarrow \pm 1.2$ (when amplifier uses loading resistor of value 1 kΩ). Example of tuning of f_p between 10 Hz and 100 Hz (the measured values are 10.7 Hz and 105 Hz and simulation gives 11.1 Hz and 114 Hz) yields value of $g_{m123} = 0.19$ and 1.1 mS. The response of BP and iAP is captured in Fig. 9 and Fig. 10, respectively.

The value of equivalent quality factor $Q = f_p/BW$ ($BW - 3$ dB bandwidth) has almost constant value varying nonessentially in a range from 0.86 to 1.02 (the nominal value is 0.88) and for full tunability the range is between 11 and 114 Hz, as it is visible in Fig. 11. Consequently, the quality factor has no dependence on tunability of the filter. The gain at the
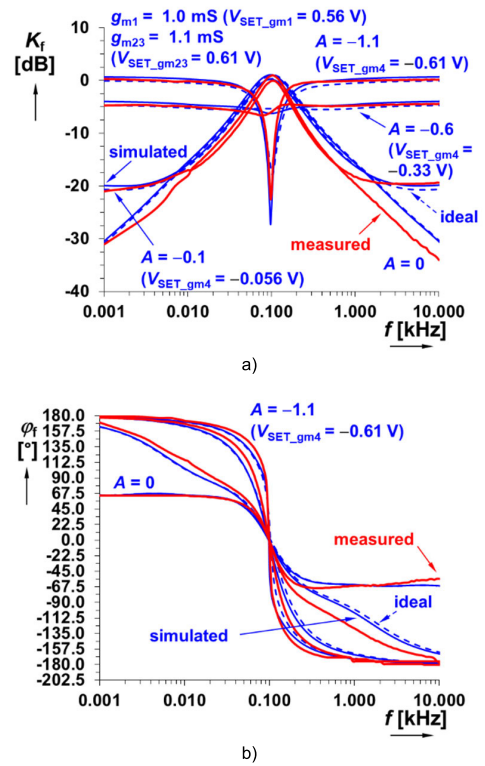
FIGURE 7. Example of important frequency responses of reconfigurable filter, shown in Fig. 1, at $f_p = 100$ Hz: a) magnitude responses, b) phase responses.
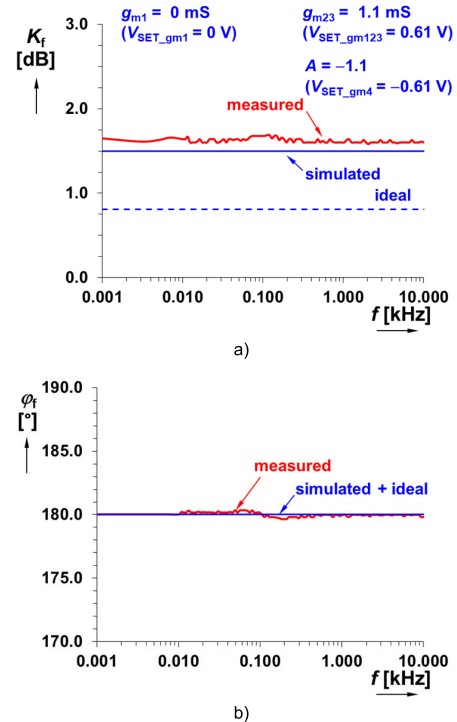
FIGURE 8. Inverting amplifier/follower responses of reconfigurable filter in Fig. 1: a) magnitude responses, b) phase responses.

center frequency can be calculated as a magnitude from (7). The power consumption of the filter reaches 40 mW (supply voltage ± 1.65 V).
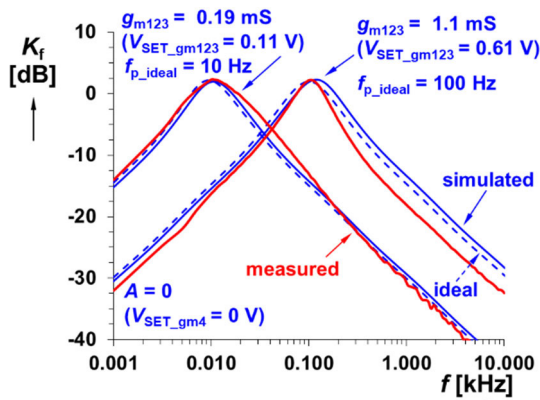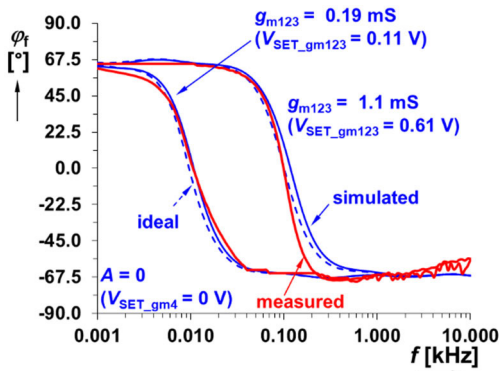
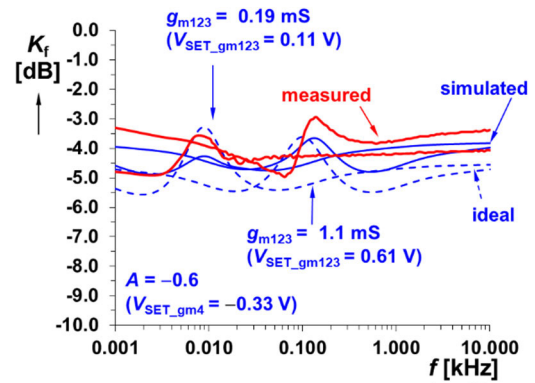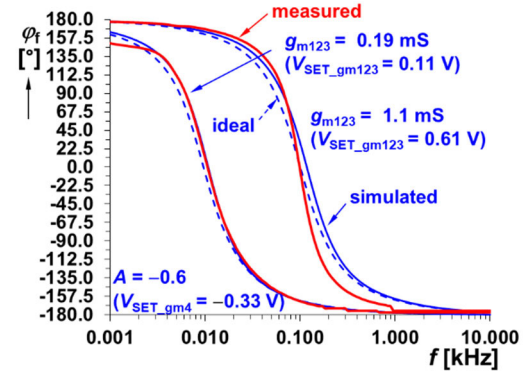**FIGURE 9.** Tuning example of band-pass responses of reconfigurable filter in Fig. 1: a) magnitude responses, b) phase responses.

FIGURE 10. Tuning example of inverting all-pass responses of reconfigurable filter introduced in Fig. 1: a) magnitude responses, b) phase responses.

The filter was tested by Monte Carlo (MC) statistical variation as well as by Process, Voltage, Temperature (PVT) and Corner analyses. Note that the CPEs are excluded from these tests because of their discrete solution (values of capacitors on IC are not available – only active devices are included on the chip). However, these tests for CPE itself are available in [27].

Fig. 12 shows the results from MC analysis (100 runs) for BP response at nominal setting (f_p = 114 Hz, V_{set_gm123} = 0.61 V, g_{m123} = 1.1 mS in the case of simulations). Statistical results indicate deviations between minimal and maximal values of center frequency f_p from 101 up to 127 Hz (the nominal value is 114 Hz with a dispersion/standard deviation up to 4.4 Hz). The minimal and maximal Q reaches values between 0.85 and 0.91 (nominal 0.88) with a standard deviation of 9.5 m.

The effects of PVT corner analysis on the performance of BP are shown in Fig. 13. The center frequency varies between 83 and 204 Hz while the quality factor is between 0.85 and 1.02. The effects of temperature variation, tested between 10 and 40 °C, have impact on the BP magnitude response (see Fig. 14). In this case, the frequency varies between 95 and 145 Hz while the value of Q is between 0.85 and 0.93. Fortunately, all possible deviations can be
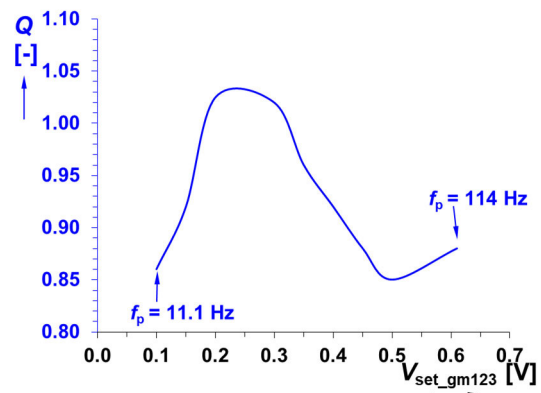
FIGURE 11. Dependence of quality factor of the BP response on driving voltage V_{set_gm123} (simulation).

easily compensated by electronically tunable features of the filter.

We have also tested iAP response on MC deviations at the same conditions because iAP is an important part of further application (frequency/phase detector). The variation of frequency f_p, where phase equals to 0°, reaches minimal and maximal values between 97 and 123 Hz (standard deviation is around 4 Hz). The worst case gain (attenuation
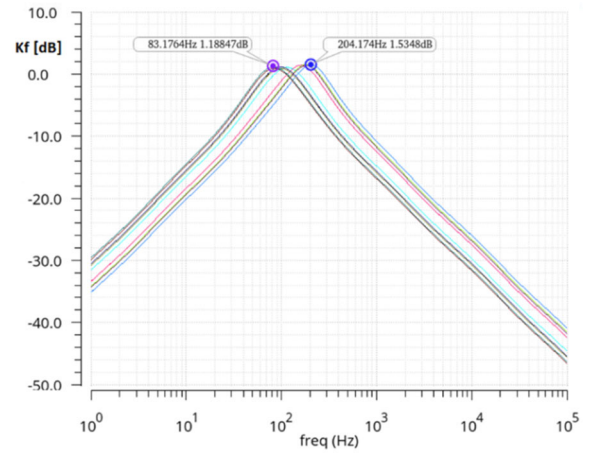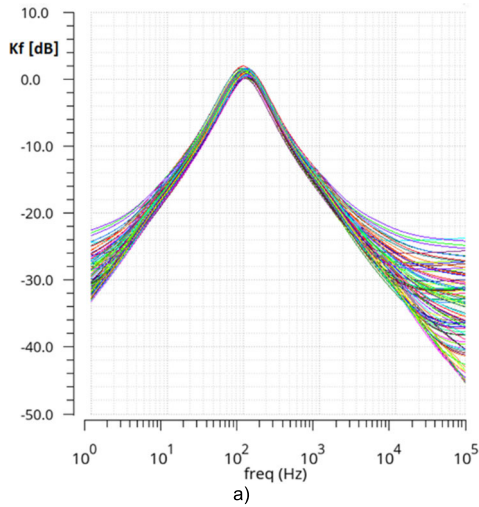
a)

b)

c)

FIGURE 12. The Monte Carlo analysis results for BP response: a) 100 runs of magnitude responses, b) histogram of statistical variations of f_p, c) histogram of statistical variations of Q.
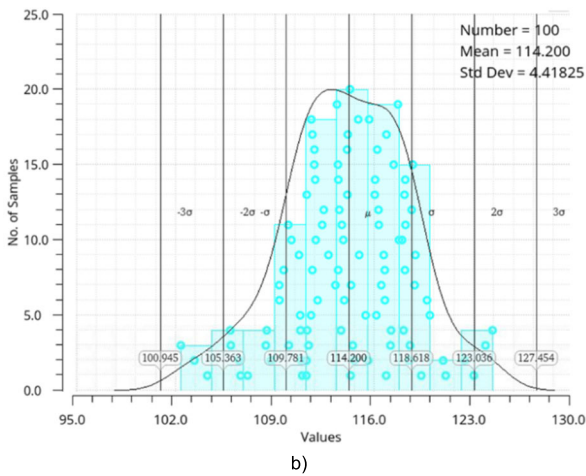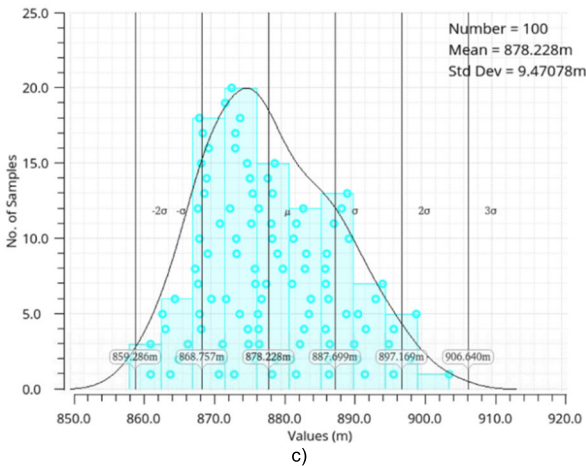

FIGURE 13. Effect of PVT corner analysis on BP magnitude response.
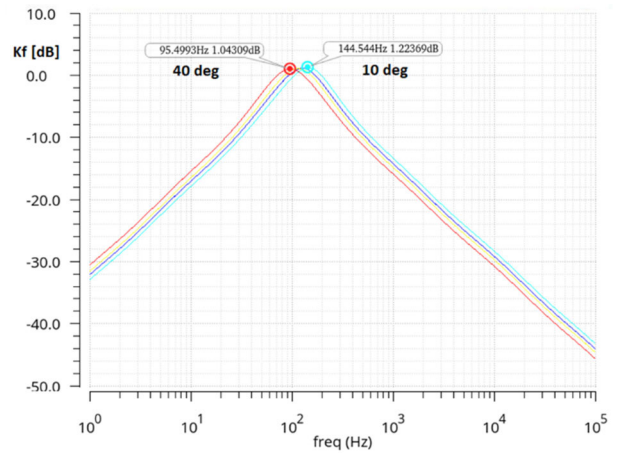
FIGURE 14. Effects of temperature analysis on BP magnitude response.

FIGURE 15. Proposed application of the frequency detector – a circuit solution.

respectively) deviation (ripple of the flat magnitude response) reaches -4.5 ± 3.5 dB (typically lower value about ± 1.5 dB). The PVT corner effects cause significantly worse results in accuracy than MC (± 5 dB in the magnitude as the largest value in the whole bandwidth). The temperature effects itself

yield maximal ± 3.5 dB variation of the gain and f_p between 93 and 137 Hz. All these results are expectable and have acceptable and easily compensable values with respect the dependence of key parameters of the filter (g_m of active elements especially) on PVT corners, temperature and statistical mismatch.

B. APPLICATION EXAMPLE OF RECONFIGURABLE FILTER – PHASE/FREQUENCY DETECTOR FOR FREQUENCY DETECTING SYSTEM OF FREQUENCY KEYING DEMODULATION

Transfer of the reconfigurable filter (see Fig. 1) offers a flat magnitude response in iAP mode useful for further applications. Such a setting (see Fig. 10) ensures operation without influence of magnitude slope changes on detection procedure in comparison with BP response. This design yields pass-band attenuation of the v_{in2} voltage about 4-5 dB with maximal magnitude change (fluctuation) 1-2 dB (between 1 Hz and 10 kHz) and center frequency of BP filter $f_p = 100$ Hz. The system of frequency detector is shown in Fig. 15. The resulting maximal output DC voltage (or signal of very low frequency – Hz, sub-Hz) of the detector is approximately determined as follows ($V_{in1,2}$ are amplitudes):

$$V_{out\_max}(\tau \ll t) \cong \frac{V_{in1}V_{in2}}{2} \cdot k \cdot R_L \cdot \cos(\varphi[rad])$$
$$\cong \frac{V_{in1}^2}{2}\left|K_f(\omega)\right| \cdot k \cdot R_L \cdot \cos(\varphi[rad]), \quad (8)$$

This equation is valid for time larger than time constant of the detector ($R_L C_L = \tau = 100$ ms). As it is visible from (8), a flat magnitude is required for precise frequency demodulation purposes. Otherwise, variation of $v_{in2}(t)$ (in the case of BP configuration of the filter in Fig. 15 – low- and high-frequency areas of magnitude slope outside of -3 dB band) cause significant impact on the value of V_{out_max} (DC). Supposing $|K_f(\omega)| \cong$ const. (due to our reconfigurable filter), the value of V_{out_max}(DC) depends on the amplitude of v_{in1} and phase shift between the input signals of the multiplier. The phase shift of the iAP filter in the detector has a complex form as can be seen in (9), as shown at the bottom of the page. Equation (9) can be substituted to (8) in order to express the dependence of V_{out_max}(DC) on input frequency.

The frequency dependence of the phase difference between the output and input wave of the reconfigurable filter (iAP response) is shown in Fig. 16. Validity of (9) for $V_{out\_max} > 0$ V limits into the range between 50 Hz and 180 Hz. Therefore, results are provided in this range.

Dependences of v_{in2} (output of the reconfigurable filter) and output DC voltage V_{out_max} on phase difference and frequency are shown in Fig. 17. The voltage amplitude v_{in1} is equal to 250 mV while v_{in2} (attenuated by 4-5 dB) reaches approximately 145 mV. The maximal value of the detected DC voltage V_{out_max} indicates phase equality between v_{in1} and v_{in2}, i.e. the input frequency having a value of center/pole frequency of current adjustment of the reconfigurable filter.

Once again, the ideal curves in Fig. 16 and Fig. 17 were obtained at simulations with controlled sources (ideal). The
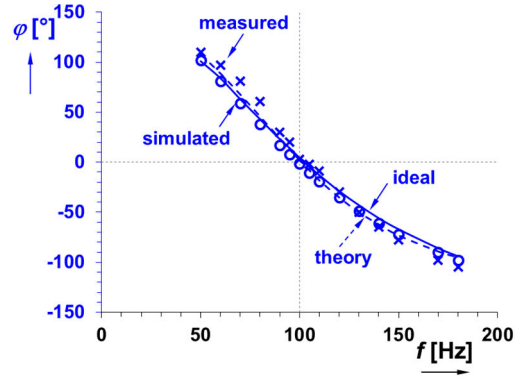

FIGURE 16. Dependence of phase difference (phase shift) of the reconfigurable filter in frequency detector on input frequency.

theoretical curves, on the other hand, were obtained by direct substitution of numeric values to the derived equations (8) and (9).

Typical examples of time responses of the system are captured in Fig. 18. These results also confirm that the maximal output voltage is reached for the input frequency identical with the center frequency of reconfigurable filter in the detector. In other words, it means alignment of the input and reference wave or wave produced at the output of the filter (iAP transfer is configured). When the maximal voltage is reached ($\cong$300-320 mV) then the input frequency is equal with the center frequency (100 Hz) and phase shift between both waves is zero. Power consumption of the application reaches 47 mW at supply voltage ±1.65 V.

The final practical application example of the proposed phase/frequency detector consists in Frequency Shift Keying (FSK) demodulation [45]. The detector can be utilized for detection of specific spectral components in slow and low-frequency signals of various natural sources (EEG, ECG, etc.) [33] or in power line communication [45]. The output of the phase detector is connected to the comparator with thresholds as it is shown in Fig. 19. The comparator uses the VDDB device from Fig. 5 b). The feedback from the output to the positive input creates an amplifier with very high (in ideal case infinite) gain. The second positive feedback using resistive dividers serves for definition of two threshold levels:

$$v_{out\_ref\_HL}(DC) \cong \left(\frac{R_2}{R_1 \| R_3 + R_2}\right) V_{DD}$$

$$v_{out\_ref\_LH}(DC) \cong \left(\frac{R_2 \| R_3}{R_2 \| R_3 + R_1}\right) V_{DD}. \quad (10)$$

The resulting values of resistors for $v_{out\_ref\_HL} = 200$ mV and $v_{out\_ref\_LH} = 150$ mV are shown in Fig. 19 (hysteresis of 50 mV used for better noise immunity). The output level varies between L state (0 V) and H state (3 V). The output

$$\varphi(\omega) = \tan^{-1}\left\{\frac{L_\alpha g_{m1}\omega^\alpha \sin\left(\frac{\pi}{2}\alpha\right) - C_\alpha L_\alpha^2 g_{m1}\omega^{3\alpha} \sin\left(\frac{\pi}{2}\alpha\right)}{A + A\left(C_\alpha L_\alpha \omega^{2\alpha}\right)^2 + L_\alpha g_{m1}\omega^\alpha \cos\left(\frac{\pi}{2}\alpha\right) + AC_\alpha L_\alpha \omega^{2\alpha}\left[4\cos^2\left(\frac{\pi}{2}\alpha\right) - 2\right] + C_\alpha L_\alpha^2 g_{m1}\omega^{3\alpha} \cos\left(\frac{\pi}{2}\alpha\right)}\right\}. \quad (9)$$
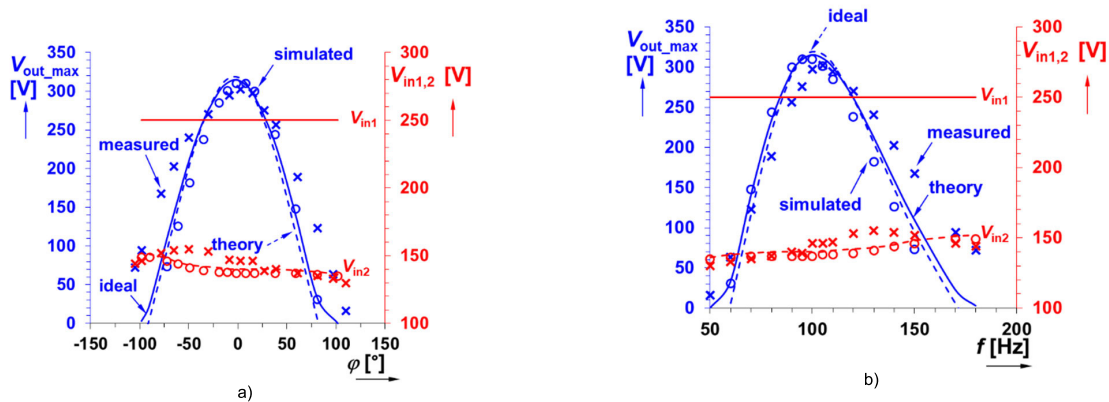
FIGURE 17. Response of the output voltage level of the reconfigurable filter and output voltage of the frequency detector on: a) phase difference, b) input frequency.
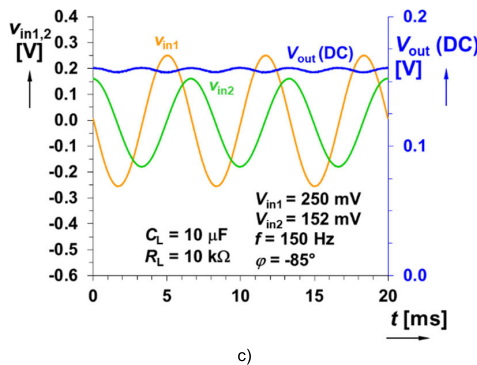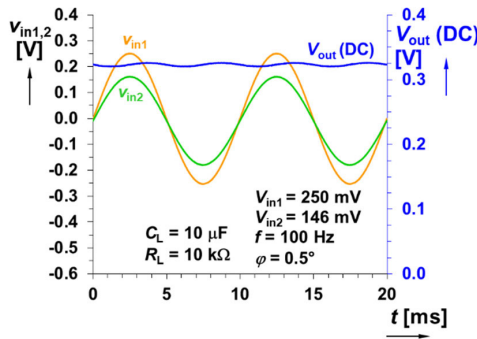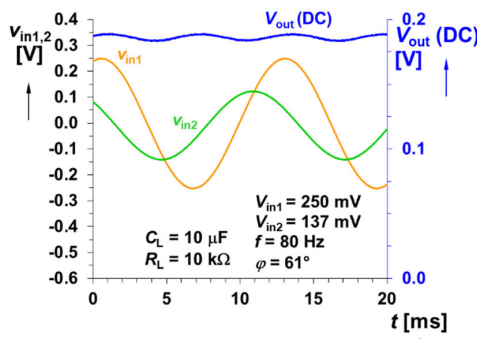

FIGURE 18. Experimental time responses of the detecting system for three different frequencies (phase shifts): a) 80 Hz, b) 100 Hz, c) 150 Hz.

drive of VDDB causes 300 mV voltage drop [43], [44]. The signaling frequency is set to 100 Hz. Based on Fig. 17 b), i.e.
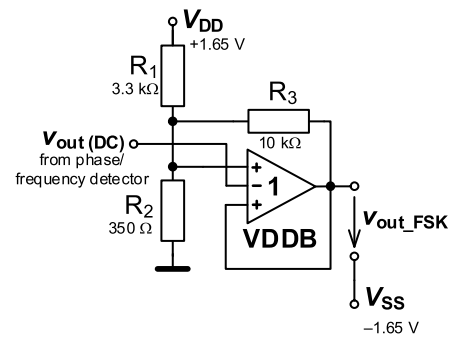

FIGURE 19. Comparator with hysteresis for signaling frequency detecting part of FSK demodulator.

knowledge of thresholds, the frequency below 80 Hz (in the experiments was set to 70 Hz) or above 130 Hz means output voltage of the frequency detector below 150 mV (below the H → L threshold level) and frequency around 100 Hz generates the maximum voltage at the output of the detector (around 300 mV) that is sufficiently above the H → L threshold level. Therefore, the presence of 70 Hz signaling frequency at the output results into state H (3 V) and frequency 100 Hz changes the output into state L (active state in this case) (0 V). It is compatible with 3.3 V logic for immediate digital processing. Please note that, in these considerations, the reference ground refers to V_{SS} (−1.65 V) at the output of the comparator. Furthermore, these features can be easily modified for specific design cases.

Employment of the frequency detector with adjustable frequency (the peak character of the response is captured in Fig. 17) is useful for decision-making systems in multi-tone modulations because frequency adjustment of the detector (f_p) and setting of comparator can be precisely adjusted (at the required value of frequency and sensitivity/selectivity) in order generate the output state (v_{out_FSK}). In other words, the change of state occurs only when the input frequency almost equals to value of the expected (set) frequency of the filter in detector. Such an example of operation is shown in Fig. 20, where the effect of additional comparator is demonstrated for evaluation of decision between two exemplary input frequencies (70 and 100 Hz) provided by the
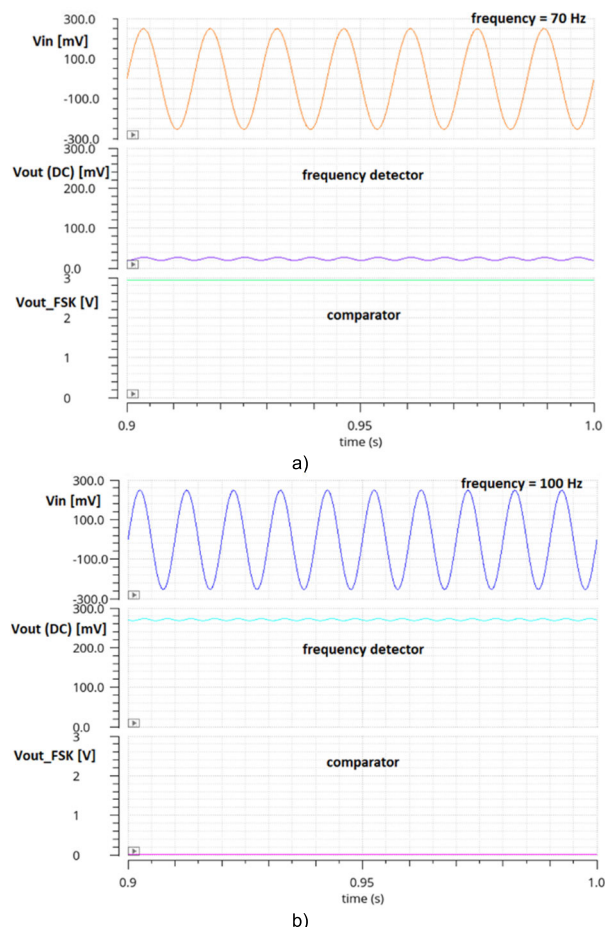
FIGURE 20. Simulated output response of signaling frequency detecting system of FSK demodulator (created by frequency detector and additional comparator) for input frequency: a) 70 Hz, b) 100 Hz.

transmitter. This application allows for us to detect specific frequency (f_p – where filter is adjusted). These distinctive features can be specified either by threshold distances (hysteresis window) of the comparator or by the slope (order, equivalent quality factor) of phase response of the iAP filter. Note that two-state demodulation (two signaling frequencies) requires two differently tuned and adjusted frequency detectors and comparators.

V. CONCLUSION

The presented concept of electronically reconfigurable filter offers a simple switchless reconfiguration of the transfer response (band-pass, inverting all-pass, special band reject and inverting direct transfer/attenuation) by a single parameter, typical for microwave structures, as well as simple electronic tuning of frequency. The proposed solution offers special transfer responses (by phase responses behavior) unavailable in standard concepts that can be beneficially utilized in further applications (adaptive frequency equalizers [46], random distortion level control [47], etc.).

Implementation of the FO resonator ensures stable operation where approximants of FO devices are connected in a grounded form. Further benefits of the implementation of the FO devices offer easy interchange of the attenuation slope of

BP response by simple replacement of the FO device having different order. The circuit has high input and low output impedance. The design was specified for center frequency 100 Hz (fitting biomedical applications) and special transfer responses (phase response of sBR and iAP settings) show good agreement between theory, Cadence simulation and experimental results in the frequency band from 1 Hz up to 10 kHz. Tuning of the filter was tested between 10 and 100 Hz (the measured values are 10.7 Hz and 105 Hz).

Features of the filter predetermine application in slow ECG or EEG signal filtering and spectral modification (adaptive distortion removal [46], [47]) as well as various different purposes. Moreover, the AP/iAP responses serve as a general active delay line in many systems for communication and measurement purposes. The presented device can be used for phase/frequency detection or synchronization (alignment) of two signals with identical frequency and phase. The tested range of detection can be found around center frequency 100 Hz between 50 and 180 Hz (phase difference when input frequencies of multiplier are identical can be detected approximately between ±100° in experimental case). The application example indicates operationability of phase/frequency detection in ten-hundreds of Hz. The maximal DC output voltage of phase/frequency detection reaches slightly more than 300 mV for alignment of waves, i.e. correspondence of input phase and frequency with set value of the filter in phase detector (100 Hz). The additional comparator together with frequency detector creates a frequency sensitive system evaluating the presence of specific frequencies for frequency shift keying demodulators or simple and precise (frequency resolution with higher accuracy than in filtering realized by a bank of filters) specific tone identification.

The presented design (theoretical idea) can be solved by different approaches and also by Field Programmable Analog Arrays (FPAAs) using different circuit topologies. Common designs using of-the-shelf (commercially available) active elements of building blocks in FPAA (standardly based on operational amplifiers) offer similar performance but the circuit and organization of passive and active elements will be more complex. It has different performances thanks to the available values and ranges (in selected way of design) of operation of fractional-order and active elements.

Theoretical concept of the system (circuit) can be created by commercially available analog devices. However, some transfer responses will not be available (e.g. for BP response when $A = 0$ or < 0, $g_m = 0$ or < 0 is unavailable in standard OTA). Standard OTAs do not provide a single bidirectional current output. Therefore, full operationability requires multiplier-based OTAs used in this work.
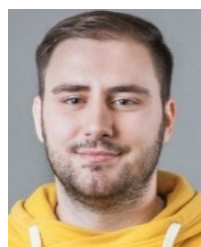
Limits of the proposed method (reconfigurability based on the sum of the response of resonator and branch of amplification) can be found in high dependence of the features of filter on accuracy of the equivalent value of CPEs and the quality of design of CPEs. Correct operation also requires special types of OTAs (based on multipliers) because zero value or positive and negative polarity of some transconductances

is required. The current design limits the tunability of the filter and operationability of frequency detecting application to tens-hundreds of Hz (especially by maximal value of g_m around 1 mS) but it is not a conceptual issue. It depends on the performances of active devices and features of CPEs that can be redesigned. The mentioned frequency range was set intentionally to slow operation following behavior of many natural biological [33] or communication systems [45].

REFERENCES

[1] Y. Sun and J. K. Fidler, "Current-mode OTA-C realisation of arbitrary filter characteristics," *Electron. Lett.*, vol. 32, no. 13, pp. 1181–1182, Jun. 1996, doi: 10.1049/el:19960807.

[2] T. Dostal, "Filters with multi-loop feedback structure in current mode," *Radioengineering*, vol. 12, no. 3, p. 6, Sep. 2003.

[3] R. Sotner, J. Petrzela, J. Jerabek, and T. Dostal, "Reconnection-less OTA-based biquad filter with electronically reconfigurable transfers," *Elektronika Ir Elektrotechnika*, vol. 21, no. 3, pp. 33–37, Jun. 2015, doi: 10.5755/j01.eee.21.3.10205.

[4] A. S. Elwakil, "Fractional-order circuits and systems: An emerging interdisciplinary research area," *IEEE Circuits Syst. Mag.*, vol. 10, no. 4, pp. 40–50, 4th Quart., 2010, doi: 10.1109/MCAS.2010.938637.

[5] L. Langhammer, J. Dvorak, R. Sotner, J. Jerabek, and P. Bertsias, "Reconnection–less reconfigurable low–pass filtering topology suitable for higher–order fractional–order design," *J. Adv. Res.*, vol. 25, no. 9, pp. 257–274, Sep. 2020, doi: 10.1016/j.jare.2020.06.022.

[6] L. Langhammer, R. Sotner, J. Dvorak, J. Jerabek, and P. A. Ushakov, "Novel electronically reconfigurable filter and its fractional-order counterpart," in *Proc. 26th IEEE Int. Conf. Electron., Circuits Syst. (ICECS)*, Genoa, Italy, Nov. 2019, pp. 538–541, doi: 10.1109/ICECS46596.2019.8965165.

[7] E. J. Naglich, J. Lee, D. Peroulis, and W. J. Chappell, "Switchless tunable bandstop-to-all-pass reconfigurable filter," *IEEE Trans. Microw. Theory Techn.*, vol. 60, no. 5, pp. 1258–1265, May 2012, doi: 10.1109/TMTT.2012.2188723.

[8] B. A. Adoum and W. P. Wen, "Investigation of band-stop to all pass reconfigurable filter," in *Proc. 4th Int. Conf. Intell. Adv. Syst. (ICIAS)*, Kuala Lumpur, Malaysia, Jun. 2012, pp. 190–193, doi: 10.1109/ICIAS.2012.6306185.

[9] T.-H. Lee, B. Lee, S. Nam, Y.-S. Kim, and J. Lee, "Frequency-tunable tri-function filter," *IEEE Trans. Microw. Theory Techn.*, vol. 65, no. 11, pp. 4584–4592, Nov. 2017, doi: 10.1109/TMTT.2017.2716931.

[10] M. Fan, K. Song, Y. Zhu, and Y. Fan, "Compact bandpass-to-bandstop reconfigurable filter with wide tuning range," *IEEE Microw. Wireless Compon. Lett.*, vol. 29, no. 3, pp. 198–200, Mar. 2019, doi: 10.1109/LMWC.2019.2892846.

[11] R. Lababidi, M. Al Shami, M. Le Roy, D. Le Jeune, and K. Khoder, "Tunable channelised bandstop passive filter using reconfigurable phase shifter," *IET Microw., Antennas Propag.*, vol. 13, no. 5, pp. 591–596, Apr. 2019, doi: 10.1049/iet-map.2018.5430.

[12] T. J. B. Freeborn, B. Maundy, and A. S. Elwakil, "Field programmable analogue array implementation of fractional step filters," *IET Circuits Devices Syst.*, vol. 4, no. 6, pp. 514–524, Nov. 2010, doi: 10.1049/iet-cds.2010.0141.

[13] G. Tsirimokou, C. Psychalinos, and A. S. Elwakil, "Fractional-order electronically controlled generalized filters," *Int. J. Circuit Theory Appl.*, vol. 45, no. 5, pp. 595–612, May 2017, doi: 10.1002/cta.2250.

[14] J. Jerabek, R. Sotner, J. Dvorak, J. Polak, D. Kubanek, N. Herencsar, and J. Koton, "Reconfigurable fractional-order filter with electronically controllable slope of attenuation, pole frequency and type of approximation," *J. Circuits, Syst. Comput.*, vol. 26, no. 10, Mar. 2017, Art. no. 1750157, doi: 10.1142/S0218126617501572.

[15] J. Dvorak, J. Jerabek, Z. Polesakova, D. Kubanek, and P. Blazek, "Multifunctional electronically reconfigurable and tunable fractional-order filter," *Elektronika ir Elektrotechnika*, vol. 25, no. 1, pp. 26–30, Feb. 2019, doi: 10.5755/j01.eie.25.1.22732.

[16] R. Sotner, N. Herencsar, J. Jerabek, J. Petrzela, and T. Dostal, "Design of integer/fractional-order filter with electronically reconfigurable transfer response," in *Proc. 24th IEEE Int. Conf. Electron., Circuits Syst. (ICECS)*, Batumi, Georgia, Dec. 2017, pp. 156–159, doi: 10.1109/ICECS.2017.8292080.

[17] N. Singh, U. V. Mehta, K. Kothari, and M. Cirrincione, "Optimized fractional low and highpass filters of $(1 + \alpha)$ order on FPAA," *Bull. Polish Acad. Sci. Tech. Sci.*, vol. 68, no. 3, pp. 635–644, Jun. 2020, doi: 10.24425/bpasts.2020.133123.

[18] G. Tsirimokou, R. Sotner, J. Jerabek, J. Koton, and C. Psychalinos, "Programmable analog array of fractional-order filters with CFOAs," in *Proc. 40th Int. Conf. Telecommun. Signal Process. (TSP)*, Barcelona, Spain, Jul. 2017, pp. 706–709, doi: 10.1109/TSP.2017.8076079.

[19] P. Bertsias, F. Khateb, D. Kubanek, F. A. Khanday, and C. Psychalinos, "Capacitorless digitally programmable fractional-order filters," *AEU-Int. J. Electron. Commun.*, vol. 78, pp. 228–237, Aug. 2017, doi: 10.1016/j.aeue.2017.04.030.

[20] A. Antoniou, "Gyrator using operational amplifier," *Electron. Lett.*, vol. 3, no. 8, pp. 350–352, Aug. 1967.

[21] R. L. Geiger and E. Sanchez-Sinencio, "Active filter design using operational transconductance amplifiers: A tutorial," *IEEE Circuits Devices Mag.*, vol. 1, no. 2, pp. 20–32, Mar. 1985, doi: 10.1109/MCD.1985.6311946.

[22] A. Adhikary, S. Sen, and K. Biswas, "Practical realization of tunable fractional order parallel resonator and fractional order filters," *IEEE Trans. Circuits Syst. I, Reg. Papers*, vol. 63, no. 8, pp. 1142–1151, Aug. 2016, doi: 10.1109/TCSI.2016.2568262.

[23] A. Adhikary, S. Sen, and K. Biswas, "Realization and study of a fractional order resonator using an obtuse angle fractor," in *Proc. IEEE Students' Technol. Symp. (TechSym)*, Kharagpur, India, Sep. 2016, Art. no. 120125, doi: 10.1109/TechSym.2016.7872667.

[24] A. Adhikary, S. Sen, and K. Biswas, "Design and hardware realization of a tunable fractional-order series resonator with high quality factor," *Circuits, Syst., Signal Process.*, vol. 36, no. 9, pp. 3457–3476, 2017, doi: 10.1007/s00034-016-0469-2.

[25] A. Adhikary, S. Choudhary, and S. Sen, "Optimal design for realizing a grounded fractional order inductor using GIC," *IEEE Trans. Circuits Syst. I, Reg. Papers*, vol. 65, no. 8, pp. 2411–2421, Aug. 2018, doi: 10.1109/TCSI.2017.2787464.

[26] G. Tsirimokou, C. Psychalinos, A. S. Elwakil, and K. N. Salama, "Electronically tunable fully integrated fractional-order resonator," *IEEE Trans. Circuits Syst. II, Exp. Briefs*, vol. 65, no. 2, pp. 166–170, Feb. 2018, doi: 10.1109/TCSII.2017.2684710.

[27] R. Sotner, J. Jerabek, L. Polak, L. Langhammer, H. Stolarova, J. Petrzela, D. Andriukaitis, and A. Valinevicius, "On the performance of electronically tunable fractional-order oscillator using grounded resonator concept," *AEU-Int. J. Electron. Commun.*, vol. 129, Feb. 2021, Art. no. 153540, doi: 10.1016/j.aeue.2020.153540.

[28] L. Kirasamuthranon, P. Wardkein, and J. Koseeyaporn, "Narrow bandwidth PLL based multiplier phase detector for PSK modulator," in *Proc. 5th Int. Conf. Comput. Commun. Syst. (ICCCS)*, Shanghai, China, May 2020, pp. 594–598, doi: 10.1109/ICCCS49078.2020.9118523.

[29] R. G. Bozomitu, V. Cehan, and R. G. Lupu, "A new CMOS differential input FM quadrature demodulator," in *Proc. 37th Int. Spring Seminar Electron. Technol.*, Dresden, Germany, May 2014, pp. 284–289, doi: 10.1109/ISSE.2014.6887609.

[30] B. Li, Y. Zhai, B. Yang, T. Salter, M. Peckerar, and N. Goldsman, "Ultra low power phase detector and phase-locked loop designs and their application as a receiver," *Microelectron. J.*, vol. 42, no. 2, pp. 358–364, Feb. 2011, doi: 10.1016/j.mejo.2010.10.010.

[31] R. Yadav and U. Kumari, "Design an optimal digital phase lock loop with current-starved ring VCO using CMOS technology," *Int. J. Inf. Technol.*, vol. 13, no. 4, pp. 1625–1631, Aug. 2021, doi: 10.1007/s41870-020-00587-6.

[32] L. F. Rahman, M. B. Reaz, M. M. Mohamad, and A. N. Hamid, "Design of low power phase detector in 0.13 μm CMOS," *J. Elect. Electron. Eng.*, vol. 10, no. 1, pp. 59–62, May 2017.

[33] S. I. Khan and S. A. Mahmoud, "Highly linear CMOS subthreshold four-quadrant multiplier for teager energy operator based sleep spindle detectors," *Microelectron. J.*, vol. 94, Dec. 2019, Art. no. 104653, doi: 10.1016/j.mejo.2019.104653.

[34] R. Sotner, L. Polak, J. Jerabek, J. Petrzela, and V. Kledrowetz, "Analog multipliers-based double output voltage phase detector for low-frequency demodulation of frequency modulated signals," *IEEE Access*, vol. 9, pp. 93062–93078, 2021, doi: 10.1109/ACCESS.2021.3092525.

[35] G. Varshney, N. Pandey, and R. Pandey, "Generalization of shadow filters in fractional domain," *Int. J. Circuit Theory Appl.*, pp. 1–18, May 2021, doi: 10.1002/cta.3054.

[36] D. Biolek, R. Senani, V. Biolkova, and Z. Kolka, "Active elements for analog signal processing: Classification, review, and new proposals," *Radioengineering*, vol. 17, no. 4, pp. 15–32, Dec. 2008.

[37] R. Senani, D. R. Bhaskar, and A. K. Singh, *Current Conveyors: Variants, Applications and Hardware Implementations*. Cham, Switzerland: Springer, 2015.

[38] J. Valsa, P. Dvořák, and M. Friedl, "Network model of the CPE," *Radioengineering*, vol. 20, no. 3, pp. 619–626, 2011.

[39] J. Valsa and J. Vlach, "RC models of a constant phase element," *Int. J. Circuit Theory Appl.*, vol. 41, no. 1, pp. 59–67, 2013, doi: 10.1002/cta.785.

[40] G. Tsirimokou, A. Kartci, J. Koton, N. Herencsar, and C. Psychalinos, "Comparative study of discrete component realizations of fractional-order capacitor and inductor active emulators," *J. Circuits Syst. Comput.*, vol. 27, no. 11, Jan. 2018, Art. no. 1850170, doi: 10.1142/S0218126618501700.

[41] R. Sotner, J. Jerabek, A. Kartci, O. Domansky, N. Herencsar, V. Kledrowetz, B. B. Alagoz, and C. Yeroglu, "Electronically reconfigurable two-path fractional-order PI/D controller employing constant phase blocks based on bilinear segments using CMOS modified current differencing unit," *Microelectron. J.*, vol. 86, pp. 114–129, Apr. 2019, doi: 10.1016/j.mejo.2019.03.003.

[42] R. Sotner, O. Domansky, J. Jerabek, N. Herencsar, J. Petrzela, and D. Andriukaitis, "Integer-and fractional-order integral and derivative two-port summations: Practical design considerations," *Appl. Sci.*, vol. 10, no. 1, p. 54, Dec. 2019, doi: 10.3390/app10010054.

[43] R. Sotner, J. Jerabek, L. Polak, R. Prokop, and V. Kledrowetz, "Integrated building cells for a simple modular design of electronic circuits with reduced external complexity: Performance, active element assembly, and an application example," *Electronics*, vol. 8, no. 5, p. 568, May 2019, doi: 10.3390/electronics8050568.

[44] J. Petrzela and R. Sotner, "New nonlinear active element dedicated to modeling chaotic dynamics with complex polynomial vector fields," *Entropy*, vol. 21, no. 9, p. 871, Sep. 2019, doi: 10.3390/e21090871.

[45] M. C. Bali and C. Rebai, "LDPC coded S-FSK modulation for power line communications," in *Proc. 4th Int. Conf. Commun. Netw. (ComNet)*, Mar. 2014, pp. 1–5, doi: 10.1109/ComNet.2014.6840922.

[46] A. H. Sayed, *Adaptive Filters*, 1st ed. Hoboken, NJ, USA: Wiley, 2008.

[47] R. Sotner, J. Jerabek, J. Petrzela, L. Langhammer, O. Domansky, W. Jaikla, and T. Dostal, "Reconnection-less reconfigurable filter and its application into adaptive circuit," in *Proc. 41st Int. Conf. Telecommun. Signal Process. (TSP)*, Athens, Greece, Jul. 2018, pp. 1–5, doi: 10.1109/TSP.2018.8441388.

ROMAN SOTNER (Member, IEEE) was born in Znojmo, Czech Republic, in 1983. He received the M.Sc. and Ph.D. degrees from Brno University of Technology, Brno, Czech Republic, in 2008 and 2012, respectively. He is currently an Associate Professor at the Department of Radio Electronics, Faculty of Electrical Engineering and Communication, Brno University of Technology. His research interests include analog circuits (active filters, oscillators, and audio), circuits in the current mode, circuits with direct electronic controlling possibilities especially and computer simulation.

LUKAS LANGHAMMER received the M.Sc. and Ph.D. degrees in electrical engineering and telecommunication from the Faculty of Electrical Engineering and Communications, Brno University of Technology (BUT), Brno, Czech Republic, in 2012 and 2016, respectively. He is currently working with the Department of Telecommunications and the Department of Radio Electronics, Faculty of Electrical Engineering and Communication, BUT. His main research interests include design and analysis of frequency filters, basic building blocks, and advanced active elements.

ONDREJ DOMANSKY was born in Hodonin, Czech Republic, in 1991. He received the M.Sc. degree in electrical engineering from the Department of Radio Electronics, Faculty of Electrical Engineering and Communications, Brno University of Technology, in 2016, where he is currently pursuing the Ph.D. degree. His research interest includes design of analog integrated circuits. Mainly on constant phase elements (CPE).

LADISLAV POLAK (Member, IEEE) was born in Štúrovo, Slovakia, in 1984. He received the M.Sc. and Ph.D. degrees in electronics and communication engineering from Brno University of Technology (BUT), Czech Republic, in 2009 and 2013, respectively. He is currently an Associate Professor at the Department of Radio Electronics (DREL), BUT. His research interests include wireless communication systems, RF measurement, signal processing, and computer-aided analysis.

• • •